Langmuir Article

pubs.acs.org/Langmuir

Dendritic Superstructures and Structure Transitions of Asymmetric Poly(L-lactide-b-ethylene oxide) Diblock Copolymer Thin Films

Shaoyong Huang,[†] Shichun Jiang,*[,‡] Xuesi Chen,[†] and Lijia An*[,†]

[†]*State Key Laboratory of Polymer Physics and Chemistry, Changchun Institute of Applied Chemistry, Chinese Academy of Sciences, Changchun 130022, P. R. China, and* [‡]*School of Materials Science and Engineering, Tianjin University, Tianjin 300072, P. R. China*

Received May 21, 2009. Revised Manuscript Received July 10, 2009

The evolution of morphologies of isothermally crystallized thin films with different thicknesses of poly(L-lactide-b-ethylene oxide) diblock copolymer was observed by optical microscopy (OM) and atomic force microscopy (AFM). Dendritic superstructures stacked with lamellae were investigated in thin films with ~200 nm to ~400 nm thickness. The lamellar structure was a lozenge- or truncated-lozenge-shaped single crystal of PLLA confirmed by AFM observations. The contour of the dendritic superstructures is hexagonal, and two types of sectors, [110] and [100], can be classified in terms of the chain-folding and crystal growth directions. These phenomena are due to the interplay of the crystallization of the PLLA block, the microphase separation of the block copolymer, and the effect of the film thickness. The growth process of the superstructure can be classified into three steps: the growth of the main branches, the growth of the secondary side branches along the main branch, and the tertiary side branches. PLLA growth rates decrease in copolymer films thinner than 1 μm. Layer−layer phase structure of the copolymer driven by the crystallization of PLLA and the microphase separation of the copolymer appears to be a key factor explaining the crystallization and morphological behavior of this system.

Introduction

Semicrystalline block copolymers with good properties, such as biodegradability, biocompatibility, innocuity, and tissue absorbability have attracted much attention because of their potential applications in environmentally friendly and medical areas. They can exhibit considerable morphology richness, arising from the two forces that can drive structure development: microphase separation between unlike blocks, which favors the formation of nanoscale domains, and crystallization of one block, which favors the formation of alternating amorphous and crystalline layers.[1] In block copolymers, when one or more block copolymer components can crystallize, a competition between microphase separation and crystallization will lead to major changes in microstructure, morphology, and complexity in the crystallization kinetics. Depending on segregation strength and the relative location of the order−disorder transition temperature T_{ODT}, the glass transition temperature T_g, and the crystallization temperature T_c, different morphologies can be generated. Either crystallization can drive structure formation for weekly segregated melt (overwriting any previous microdomain structure) or crystallization can be confined within the copolymer microdomain structure for strongly segregated systems or homogeneous systems.[2−6]

Meanwhile, decreasing film thickness dramatically alters the molecular mobility,[7−12] glass transition temperatures,[13,14] and segmental orientation[15,16] of semicrystalline polymers. These factors influence the transport of chain segments to the growth front of crystallizing lamella, resulting in growth rates, degrees of crystallinity, and morphologies that are different from those of bulk crystals. A number of previous studies have reported the observations of diffusion-limited crystal growth in thin polymer films.[17−24] These previously observed diffusion-limited morphologies include dense-branched morphologies, dendrites, and fractal structures.

It has been confirmed that PLLA16k-b-PEO5k diblock copolymer is weekly segregated,[25,26] and the melting and crystalline

*Corresponding author. E-mail:scjiang@tju.edu.cn (S.J.); ljan@ciac.jl.cn (L.A.).

(1) Loo, Y.-L.; Register, R. A.; Ryan, A. J. *Macromolecules* **2002**, *35*, 2365–2374.
(2) Rangarajan, P.; Register, R. A.; Adamson, D, H.; Fetters, L. J.; Bras, W.; Naylor, S.; Ryan, A. J. *Macromolecules* **1995**, *28*, 1422–1428.
(3) Ryan, A. J.; Hamley, I. W.; Bras, W.; Bates, F. S. *Macromolecules* **1995**, *28*, 3860–3868.
(4) Nojima, S.; Toei, M.; Hara, S.; Tanimoto, S.; Sasaki, S. *Polymer* **2002**, *43*, 4087–4090.
(5) Reiter, G.; Castelein, G.; Sommer, J. U.; Röttele, A.; Thurn-Albrecht, T. *Phys. Rev. Lett.* **2001**, *87*, 226101–226104.
(6) Hamley, I. W.; Castelletto, V.; Castillo, R. V.; Müller, A. J.; Martin, C. M. *Macromolecules* **2005**, *38*, 463–472.
(7) Bingbing, Li; Herve, Marand; Alan, R. Esker *J. Polym. Sci.: Part B: Polym. Phys.* **2007**, *45*, 3300–3318.
(8) Forrest, J.; Dalnoki, V.; Stevens, J.; Dutcher, J. *Phys. Rev. Lett.* **1996**, *77*, 2002–2005.
(9) Kawana, S.; Jones, R. *Phys. Rev. E* **2001**, *63*, 021501–021506.
(10) Miyazaki, T.; Nishida, K.; Kanaya, T. *Phys. Rev. E* **2004**, *69*, 06183–8.
(11) Zheng, X.; Sauer, B. B.; Van Alsten, J. G.; Schwarz, S. A.; Rafailovich, M. H.; Sokolov, J.; Rubinstein, M. *Phys. Rev. Lett.* **1995**, *74*, 407–410.
(12) Frank, B.; Gast, A. P.; Russell, T. P.; Brown, H. R.; Hawker, C. *Macromolecules* **1996**, *29*, 6531–6534.
(13) Forrest, J. A.; Dalnoki-Veress, K.; Dutcher, J. R. *Phys. Rev. E* **1997**, *56*, 5705–5716.
(14) Mattson, J.; Forrest, J. A.; BOrjesson, L. *Phys Rev E* **2000**, *62*, 5187–5200.
(15) Frank, C. W.; Rao, V.; Despotopoulou, M. M.; Pease, R. F. W.; Hinsberg, W. D.; Miller, R. D.; Rabolt, J. F. *Science* **1996**, *273*, 912–915.
(16) Despotopoulou, M. M.; Frank, C. W.; Miller, R. D.; Rabolt, J. F. *Macromolecules* **1996**, *29*, 5797–5804.
(17) Mareau, V. H.; Prud'homme, R. E. *Macromolecules* **2002**, *35*, 5338–5341.
(18) Mareau, V. H.; Prud'homme, R. E. *Macromolecules* **2003**, *36*, 675–684.
(19) Mareau, V. H.; Prud'homme, R. E. *Macromolecules* **2005**, *38*, 398–408.
(20) Mareau, V. H.; Prud'homme, R. E. *Polymers* **2005**, *46*, 7255–7265.
(21) Reiter, G.; Sommer, J.-U. *Phys. Rev. Lett.* **1998**, *80*, 3771–3774.
(22) Reiter, G.; Castelein, G.; Sommer, J.-U. *Phys. Rev. Lett.* **2001**, *86*, 5918–5921.
(23) Ferreiro, V.; Douglas, J. F.; Warren, J A.; Karim, A. *Phys. Rev. E* **2002**, *65*, 042802–042804.
(24) Beers, K. L.; Douglas, J. F.; Amis, E. J.; Karim, A. *Langmuir* **2003**, *19*, 3935–3940.
(25) Huang, S.; Jiang, S.; An, L.; Chen, X. *J. Polym. Sci. Part B: Polym. Phys.* **2008**, *46*, 1400–1411.
(26) Sun, J. R.; Hong, Z. K.; Yang, L. X.; Tang, Z. H.; Chen, X. S.; Jing, X. B. *Polymer* **2004**, *45*, 5969–5977.

temperatures of the PLLA block are higher than those of the PEO block. The PLLA block crystallizes first and produces a specific morphology during the cooling process. As a result, the initial melt morphology due to the weak microphase separation in the block copolymer can be sequentially overwritten by the crystallization of the PLLA block. The crystallization kinetics of the PLLA block can be dramatically affected by the presence of the other block and the crystallization temperature, and the magnitude of the effect is a function of thermodynamic repulsion.[27] Such modifications depend, among other controlling parameters, on segregation strength, crystallization temperature, and molecular weight of the block components. The crystallization and morphological behaviors in thin films of asymmetric PLLA-b-PEO copolymers were investigated. We will consider the effects of microphase separation on the crystallization and morphological behaviors in three factors: crystallization temperature, film thickness, and the molecular weight of the block components. The common criteria for breakout crystallization of the used samples is $T_c > T_{ODT} > T_g$. In the present study, the crystallization temperature (T_c) of PLLA block is higher than the glass transition temperature of PEO block (T_g), and the order-to-disorder transition temperature (T_{ODT}) of the copolymers. Hexagonal dendritic morphology, which is stacked with PLLA single crystals, was observed in PLLA-b-PEO copolymer thin films of 200 nm to 400 nm in thickness.[28,29] The crystallization kinetics of the thin films and the thermal stability of the morphology are also investigated using time-resolved optical microscopy.

Experimental Section

Materials. PLLA-b-PEO diblock copolymers were synthesized according to the ref 26. The prepared samples were classified by GPC and purified by a sedimentation method. The asymmetric diblock copolymers were named as PLLA16k-B-PEO5k and PLLA30k-b-PEO5k. 16k, 30k, and 5k are the number average molecular weight of PLLA16k, PLLA30k, and PEO5k blocks, respectively. The PLLA31k homopolymer was purchased from Aldrich Company and used without further purification. The characteristics of these materials used are shown in ref 25.

Sample Preparation. All samples for crystallization were prepared by spin-coating chloroform solutions with different polymer concentrations on clean silicon wafers. In order to receive thin films of various thicknesses, we changed the concentration of the copolymer solutions to 0.2%, 0.3%, and 0.5% (wt%), and the rotation speed of the spin-coating to 1000 rpm, 1500 rpm, 2500 rpm, respectively; the rotation time was 30 s. The substrates were covered completely by the copolymers. After the solvent was evaporated completely, the samples were heated to 180 °C (for copolymers) or 200 °C (for the PLLA homopolymer) for complete melting, using a Linkam TMS94 hot stage (coupled with optical microscopy), and then cooled to an isothermal crystallization temperature ($T_{c,x}$, 90−125 °C) at −30 °C/min. Finally, the temperature was decreased rapidly to room temperature. The melting and annealing processes were carried out in a nitrogen atmosphere. The prepared samples were for OM and AFM observations. Film thicknesses were measured by AFM.

Optical Microscopy. The morphology and the thermal stability of copolymer thin film observations were performed with a Leica optical microscope (Leica, LM_1-113, Japan), equipped with a hot-stage (Linkam TMS94) and a Panasonic CCD camera system.

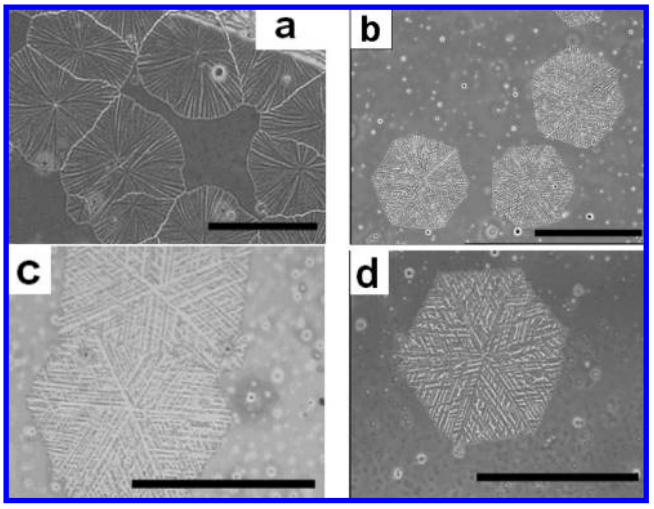

Figure 1. Morphologies of PLLA16k-b-PEO5k copolymer thin films crystallized at (a) 90 °C, (b) 100 °C, (c) 110 °C, and (d) 120 °C. The thickness of the films is ~220 ± 30 nm. The bar corresponds to 100 μm.

Atomic Force Microscopy. The surface morphologies of PLLA-b-PEO copolymer and PLLA homopolymer thin films were observed employing atomic force microscopy (Seiko Instruments Inc., SPA300HV with a SPI3800N controller). A 150 μm scanner and SiN_4-candilevers with a spring constant of 42N/M were applied for tapping mode imaging. Both height and phase images were recorded simultaneously using the retrace signal at room temperature. The film thickness was determined from the height image.

Results and Discussion

Crystal Morphology. *Influence of Crystallization Temperature*. Optical microscopic images of PLLA16k-b-PEO5k copolymer thin films isothermally crystallized at different temperatures for a very long time are shown in Figure 1. Dendritic morphologies are formed. At 90 °C shown in Figure 1a, dendritic morphologies with discal contours were observed, which were formed with many radial branches. Dendritic superstructures with hexagonal contours were observed in thin films crystallized above 100 °C, as seen in Figure 1b−d. The images show that the dendritic morphology is composed of six sectors with some overgrowth lamellae. The change of the morphology contour with crystallization temperature shown in Figure 1 is ascribed to the temperature dependence of nucleation and growth, the addition of the PEO block, and phase separation between the two unlike blocks during the crystallization of PLLA.

To visualize the detailed crystalline morphologies of the PLLA16k-b-PEO5k copolymer, tapping mode AFM was employed. The AFM images are shown in Figure 2. For the thin films crystallized at lower temperatures, the number of main branches in every crystalline morphology is higher than that of identical films crystallized at higher temperatures. Lozenge-spiral dislocation (right arrow in the phase images at 120 °C), lozenge-multilayer (arrow in the images at 100 °C), or truncated-lozenge multilayer (left arrow in the images at 120 °C) was formed in the growth direction perpendicular to the lamellae. The size of lamellae increases with crystallization temperature. The *d* spacing of lamellae of 10−12 nm in thickness is identical with that of the PLLA single crystal. The crystalline morphology is formed by stacking flat on growing lamellae in the thin film. A lozenge-shaped single crystal with screw dislocation of PLLA has been reported in a thin film of PLLA or its copolymers whose thickness

(27) Glicksman, M. E.; Koss, M. B. *Phys. Rev. Lett.* **1994**, *73*, 573–576.
(28) Lu, Y.; Beckermann, C. 2002 ASME International Mechanical Engineering Congress and Exposition, Nov 17-22, HTD-Vol.372-5, 2002, New Orleans, Louisiana.
(29) Beckermann, C.; Li, Q.; Tong, X. *Sci. Technol. Adv. Mater.* **2001**, *2*, 117–126.

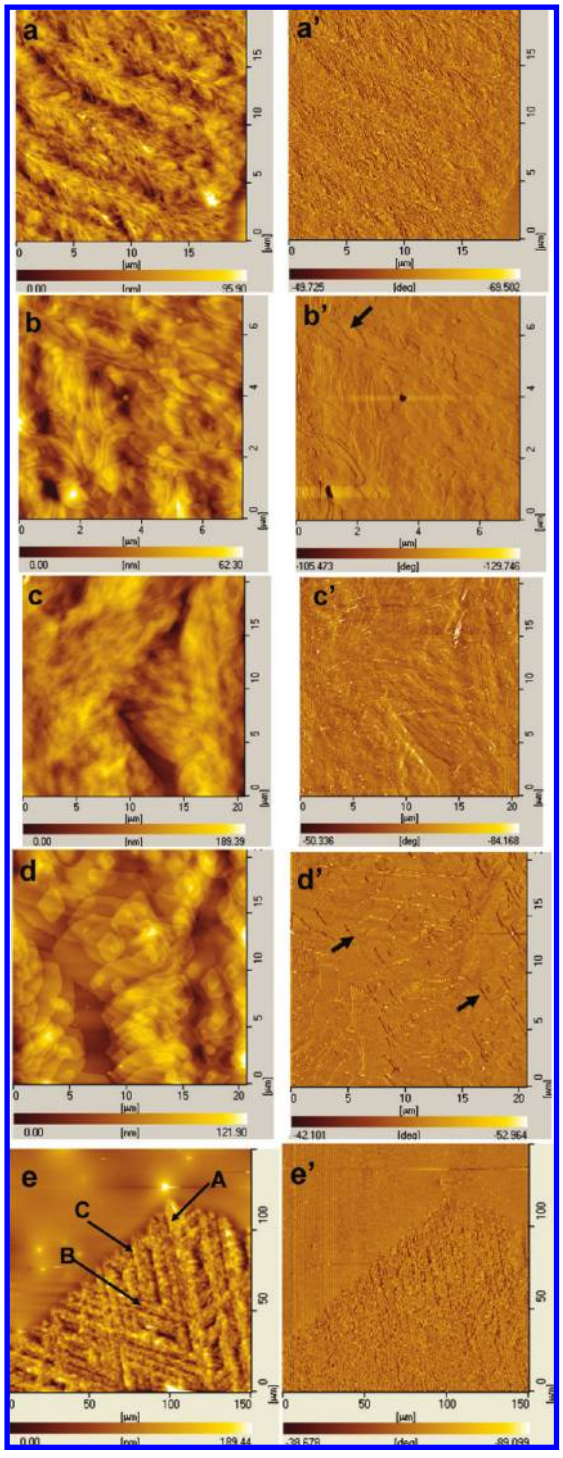

Figure 2. AFM height (left column) and phase (right column) images of PLLA16k-b-PEO5k copolymer thin films crystallized at (a) 90 °C, (b) 100 °C, (c) 110 °C, (d) 120 °C, and (e) 110 °C. A, the main branch; B, the secondary side branch; C, the tertiary side branch.

is less than 100 nm.[25,26,30−34] However, the special crystalline morphology of hexagonal dendrite stacked with PLLA single crystals has never been reported. The dependence of crystalline morphology on T_c can be explained by supercooling and phase separation. For PLLA homopolymer thin films with identical thickness, spherulitic morphologies are formed in the temperature range from 90 to 120 °C. For PLLA-b-PEO copolymer thin films, microphase separation is driven by the crystallization of the PLLA block formed layer−layer structure (that is to say alternate PLLA- and PEO-rich domains). Furthermore, the size of the PLLA layer is quite smaller than the film thickness, which is tens or a hundred nanometers as determined by AFM. At lower T_c, the supercooling is larger, many nuclei are formed rapidly, then lots of small PLLA single crystals grow up, and star shaped dendritic morphologies are observed at 90 °C in Figures 1a and 2a. While at higher T_c, the number of elementary nuclei is relatively small; secondary nucleation is important in the crystallization process, and as a consequence, dendritic morphologies composed with main branches, secondary sidebranches, and tertiary side branches were formed as shown in Figures 1b−d and 2b−d. Furthermore, the structure in the areas of the films that appears not to contain dendritic structures was amorphous PEO and PLLA blocks. At high crystallization temperature, it is difficult for nucleation to occur, especially for homogeneous nucleation. Once nucleus was formed, with crystallization procedures by diffusion and ordering of PLLA chains. In the crystallization process, the PLLA block can preferentially attach on the growth front, and then the accumulation of amorphous components in the vicinity of the dendrites will prevent the nucleation and crystallization in the areas.

Influence of Film Thickness. Figure 3 shows typical OM images of PLLA16k-b-PEO5k thin films with different thicknesses crystallized at 110 °C. Spherulites are formed in ~10 μm thick films as shown in Figure 3a, while for the films in the thickness range from 1 μm to ~200 nm, dendritic morphologies were observed, as seen in Figure 3b−e. Maltese cross-extinction was not found in the center of any crystalline morphology in the films with the thickness range from 1 μm to ~200 nm, indicating that the optic axis (the chain axis) is normal to the plane of the film. The morphologies in Figure 3b−e are discal dendritic as confirmed from AFM observations. Most of the fringe frames of the morphologies formed in thin films with the thickness from 200 nm to 400 nm are hexagonal as shown in Figure 3c−e, and the size of the hexagonal morphologies is about 100 μm. The hexagonal dendritic morphologies were composed of six sectors. In the film with 115 nm thickness (Figure 3f), lozenge-shaped lamellae were formed. The stack and the growth of PLLA single crystals are oriented as shown in Figure 3f. The PLLA single crystal in homopolymer or copolymer thin films has been reported,[25,26,30] but a hexagonal superstructure has never been observed. We speculated that the formation of the special superstructure was the interplay of crystallization, microphase separation between the unlike blocks, and diffusion limitation in the thin film.[7,17−24] The diffusion and crystallization processes of the PLLA block drove microphase separation between the unlike blocks and the formation of concentration gradient of PLLA. Moreover, the average growth rate was nearly linear, and it was easy to form dendrites not spherulite in thin films.[19−22] As a result, the hexagonal contour morphology was probably formed. The formation of the dendritic morphologies stacked with PLLA single crystals in PLLA-b-PEO thin films ranging from 1 μm to 200 nm in thickness is related with the phase structure and its evaluation during the crystallization process, and the mechanism will be further discussed in the following paragraph.

Influence of Component. Figure 4 shows the effect of the component on crystalline morphology. It can be seen that the

(30) Müller, A. J.; Arnal, M. L.; Balsamo, V. *Lect. Notes Phys.* **2007**, *714*, 229–259.
(31) Kikkawa, Y.; Abe, H.; Iwata, T.; Inoue, Y.; Doi, Y. *Biomacromolecules* **2001**, *2*, 940–945.
(32) Fujita, M.; Doi, Y. *Biomacromolecules* **2003**, *4*, 1301–1307.
(33) Yang, J.; Zhao, T.; Zhou, Y.; Liu, L.; Li, G.; Zhou, E.; Chen, X. *Macromolecules* **2007**, *40*, 2791–2797.
(34) Fujita, M.; Doi, Y. *Biomacromolecules* **2003**, *4*, 1301–1307.

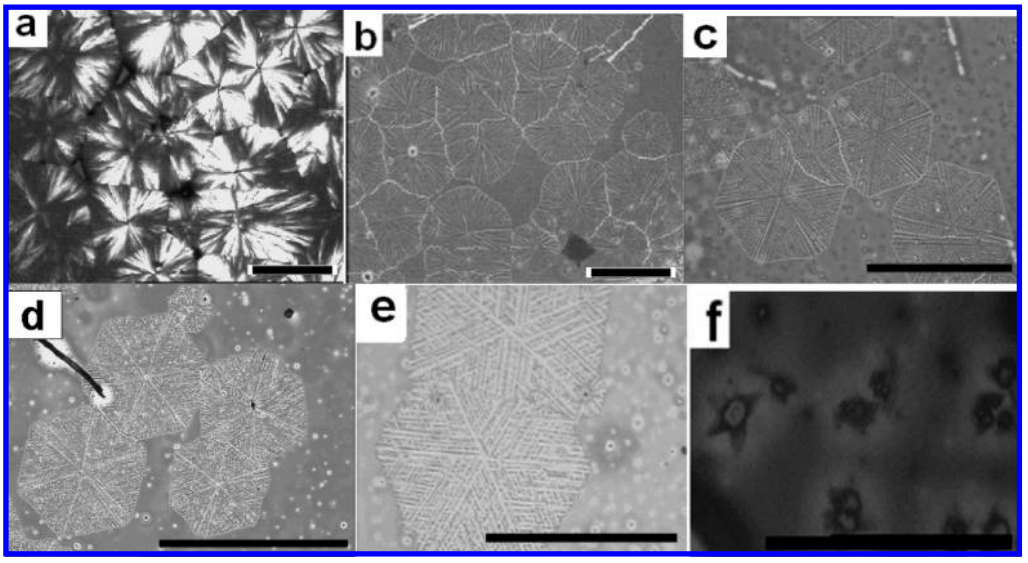

Figure 3. Morphologies of PLLA16k-b-PEO5k copolymer thin films crystallized at 110 °C. Film thickness: (a) ~10 μm, (b) 1 μm, (c) ~400 nm, (d) ~300 nm, (e) 220 nm, and (f) 115 nm. The bar corresponds to 100 μm.

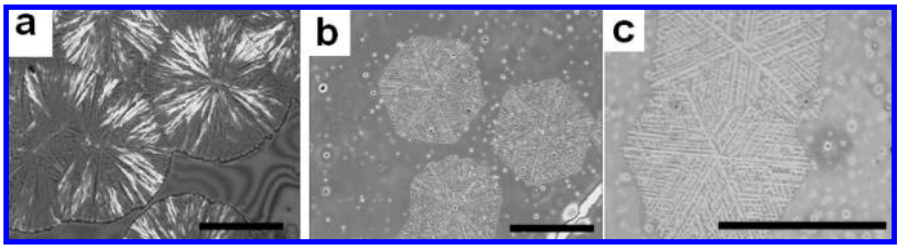

Figure 4. Morphologies of (a) PLLA31k homopolymer, (b) PLLA30k-b-PEO5k, and (c) PLLA16k-b-PEO5k copolymer films with the thickness of ~220 ± 30 nm crystallized at 110 °C. The bar corresponds to 100 μm.

morphology changes from spherulite (Figure 4a) to dentrite (Figure 4b) and to dendrite with hexagonal contour (Figure 4c) with increasing volume fraction of PEO. The effect of PEO blocks on the crystallization and morphological behaviors of PLLA blocks is multiple. The melting points of the PLLA block in PLLA-b-PEO copolymers decrease with decreasing fraction;[25,26] therefore, the degree of supercooling ($\Delta T = T_m - T_c$) decreases with increasing PEO fraction. Then at 110 °C, at the low temperature range of crystallization for PLLA homopolymer, spherulite is formed (Figure 4a), while for PLLA30k-b-PEO5k and PLLA16k-b-PEO5k copolymers, it is high temperature range of crystallization; as a result, dendritic morphologies are observed (Figure 4b,c). It is common to form dendritic morphology[17−24] in thin film, and this has been discussed. Meanwhile, the volume fractions of the PLLA block and the total degree of polymerization (N) are different in the three samples in Figure 4a−c, and the segregated strength of microphase separation between the two blocks is different. As a result, the number of nuclei in every area and the density of the branches in the PLLA30k-b-PEO5k copolymer thin film are larger than those in PLLA16k-b-PEO5k. That is to say, as the volume fraction of the PEO block increases, the effect of PEO on the crystalline morphology increases. It affects the crystallization of the PLLA block in three ways. First, the number of PLLA blocks decreases in thin films of the same thickness. Second, the diffusion of the PLLA block becomes more difficult because of the increase in the volume fraction of PEO. Third, the size of microstructure driven by phase separation may be larger. As a consequence, we got the evolution of crystalline morphology in copolymer thin films with different components in Figure 4. The morphologies were observed after annealing to room temperature, as a result, the PEO blocks might also crystallize, but the WAXD research has confirmed that it is quite difficult for the PEO block to crystallize in such asymmetric block copolymers because of the strong confinement from microphase separation.[25]

We are not sure that the crystalline morphologies observed by OM and AFM in Figures 1−4 are those created during crystallization of the PLLA block. It is possible that some of the patterns are formed by rearrangements after crystallization (or rearrangements of already crystallized parts while new material is still crystallizing). In order to confirm whether the morphologies observed are those formed during crystallization, an in situ OM experiment for isothermal crystallization was carried out. Figure 5 shows the polarized optical microscopic images of morphological growth of the PLLA16k-PEO5k copolymer thin film isothermally crystallized at 110 °C. At 12 min, as shown in Figure 5a, the dendritic morphologies with hexagonal contours similar to those in Figures 1 and 3 are observed. From Figure 5b−d, we can see that the thickness and the size of the crystalline morphologies grew thicker and larger, but the crystalline morphology observed by OM is similar all the time, indicating the morphologies observed are created during crystallization.

The thickness of the copolymer film in the experiment is 1 μm−200 nm; as a result, the substrate may influence the crystalline morphology. It is possible that one of the blocks adsorbs strongly to the substrate. If this is the case, then the strong attachment of one block to the substrate can control the morphology. PLLA-b-PEO copolymers and PLLA/PEO blends belong to a weakly

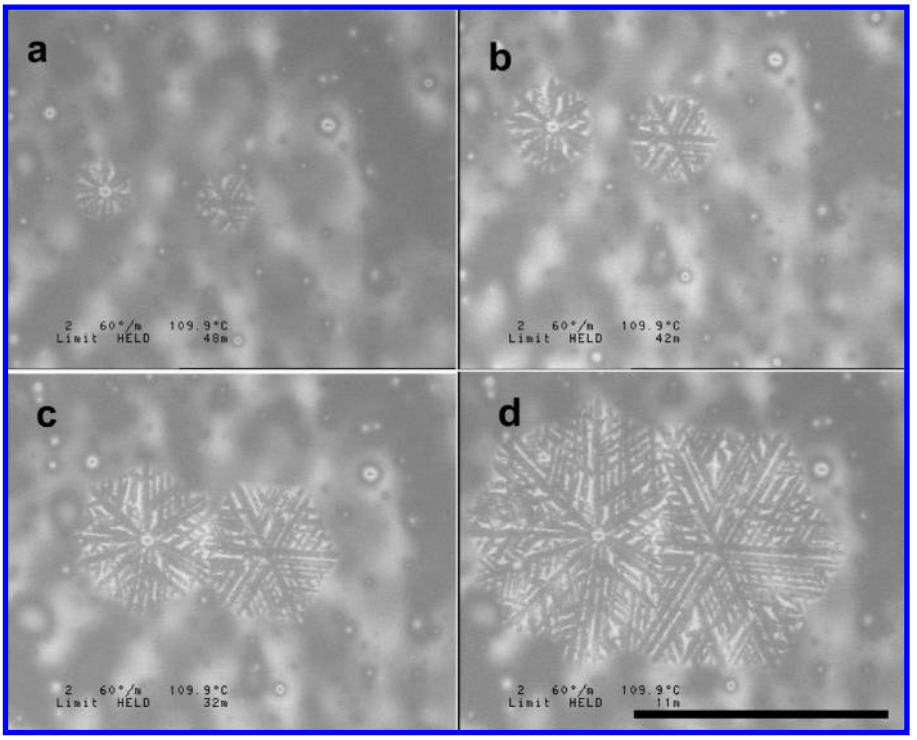

Figure 5. Polarized optical microscopic images of PLLA16k-PEO5k thin films crystallized at 110 °C at 12 min, 18 min, 28 min, and 49 min after completely melting at 180 °C. The bar corresponds to 100 μm.

segregated system; PEO and PLLA could not be strongly segregated or have one of them strongly adsorbed to the substrate.[26,33] Meanwhile, the film thickness range from 1 μm to 200 nm is much larger than the size of the extended copolymer chain; therefore, the effect of substrate on morphology is neglectable.

How are the special dendritic morphologies stacked with the PLLA single crystal formed in the PLLA-b-PEO copolymer thin films? The PLLA-b-PEO copolymers in our experiment are asymmetric, the fractions of the PEO block are about 14% and 25%, and the PLLA and PEO blocks in the copolymer are miscible at melting state as shown in Figure 6a. The crystallization of the PLLA block, microphase separation between PLLA and PEO blocks, and phase transformation of PLLA from amorphous to crystalline phase take place synchronously. The process leads to the formation of new phase distribution and microstructure, which will affect the crystallization behavior and its morphology. It is difficult for the PLLA homopolymer to form single crystals in thin films of more than 200 nm thickness. How is the dendritic morphology stacked with single crystals formed? We speculated that it is the interplay of crystallization, microphase separation between the unlike blocks, and the effect of thin films. Alternate layer−layer structure may be formed driven by microphase separation and phase transformation. We have confirmed that the PLLA-b-PEO copolymers are disordered[25,26] at melt state; therefore, the film structure of the PLLA-b-PEO copolymer can be schematically depicted in Figure 6a. In the isothermal crystallization process, the PLLA block can preferentially attach on the growth front around the apexes. Meanwhile, the accumulation of amorphous components including amorphous PLLA and PEO blocks in the vicinity of the protrusions reduces the supersaturation of the PLLA block and prevents further growth in the immediate vicinity of the trailing edge; therefore, the growth and stack of lamellae were oriented. As the crystallization and growth of the PLLA block take place, microphase separation takes place; most of the amorphous phase is onto the surface of

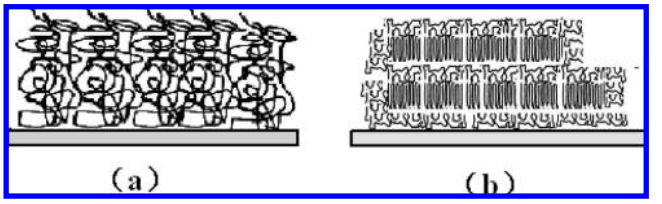

Figure 6. Schematic representations for PLLA-b-PEO thin film (a) disordered phase at melting state and (b) layer−layer structure driven by crystallization of PLLA block and microphase separation.

the crystalline PLLA, and the crystallization and microphase separation both drive the formation of PLLA-rich and PEO-rich areas. As a result, the size of the PLLA domains was confined within 100 nm domains, and the layer−layer structure[1,30,31,34−37] might be formed as shown in Figure 6b. One layer is the crystalline PLLA phase, and the alternate layer is the amorphous phase including PEO and amorphous PLLA. Only in this way, lozenge- or truncated-lozenge-shaped single crystals of PLLA can be formed. During the annealing process and at room temperature, parts of the PEO blocks may crystallize, but the effect on change of the final morphology is neglectable. It is because its volume fraction is small and because its crystallization will be confined within the microdomains formed by microphase separation of the copolymers, crystallization, and vitrification of PLLA blocks.

To visualize the morphology of the PLLA-b-PEO copolymer thin film from the melt, time-resolved imaging of the melting process of the crystalline morphology in the thin film was carried out by temperature-controlled OM equipped with a heating stage. The heating rate was 1 °C/min. Figure 7 shows the time-dependent changes in surface morphology of PLLA-b-PEO thin films

(35) Chung, H.; Composto, R. J. *Phys. Rev. Lett.* **2004**, *92*, 185704–185707.
(36) Wang, H.; Composto, R. J. *J. Chem. Phys.* **2000**, *113*, 10386–10397.
(37) Chung, H.; Wang, H.; Composto, R. J. *Macromolecules* **2006**, *39*, 153–161.

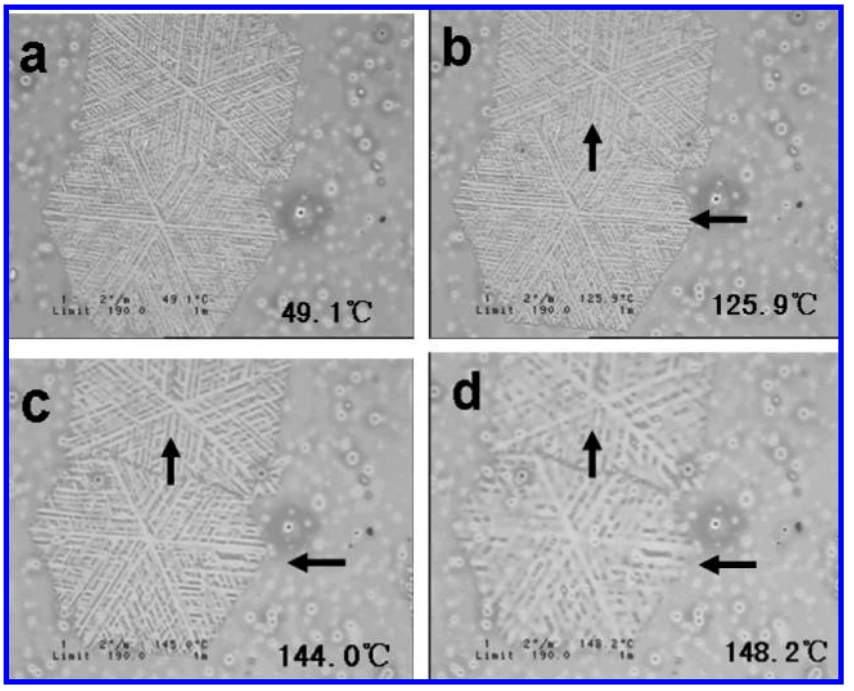

Figure 7. Optical micrographs of the melting process of PLLA16k-b-PEO5k thin film (~220 nm in thickness, isothermally crystallized at 110 °C).

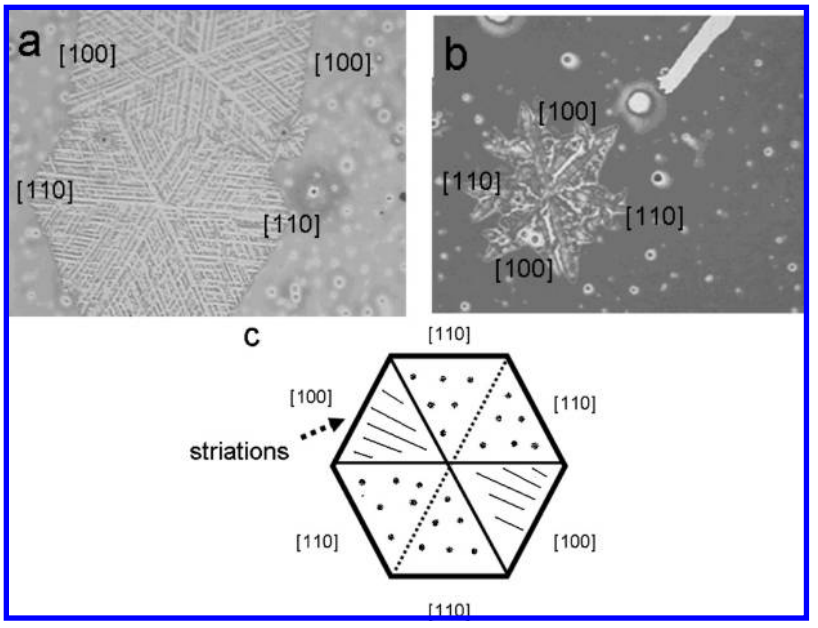

Figure 8. Two types of sectors [110] and [100] were classified in terms of chain-folding and crystal growth directions in a hexagonal superstructure of PLLA-b-PEO copolymer thin films isothermally crystallized at (a) 110 °C and (b) 125 °C. (c) Schematic representation of the hexagonal superstructure of PLLA-b-PEO copolymer thin film.

with 220 nm thickness during isothermal crystallization at 110 °C. At 125.9 °C, the sectors labeled by arrows in Figure 7b started melting. When the temperature reached 144 °C as shown in Figure 7c, the sectors next to the labeled ones began to melt, and at 148.9 °C as shown in Figure 7d, the sectors labeled by arrows were illegible and we could not see the crystalline morphology. However straits in the sectors next to the labeled ones could be seen, which indicated that the thermal stability of the sectors was different.

For PLLA crystals grown in spin-coated thin films on solid surfaces,[19,38] four symmetrically disordered sectors in the hexagonal superstructure are formed, and they can be classified into two sectors, [100] and [110], in terms of chain-folding and crystal growth directions.[39] From the growth process in Figure 7 and the dendritic morphologies with hexagonal contours formed in thin films with ~200−400 nm thickness in Figures 1−3, the hexagonal superstructure is composed of two different sectors, as shown in Figure 8a−b. Figure 8c schematically represents the hexagonal

(38) Olsen, B. D.; Segalman, R. A. *Macromolecules* **2006**, *39*, 7078–7083.

(39) Kikkawa, Y.; Abe, H.; Iwata, T.; Inoue, Y.; Doi, Y. *Biomacromolecules* **2002**, *3*, 350–356.

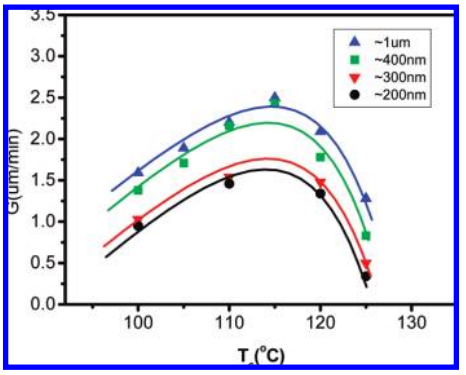

Figure 9. Growth rate G (μm/min) of PLLA16k-b-PEO5k copolymer thin films, as a function of the isothermal crystallization temperature (T_c (°C)), in linear scale.

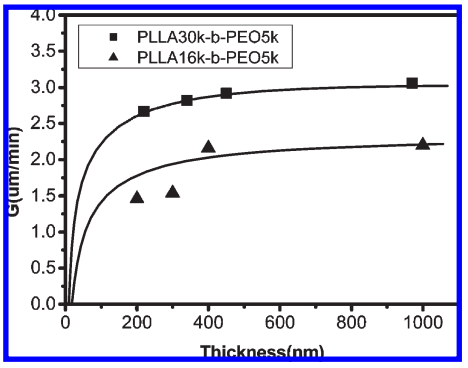

Figure 10. Radial growth rate G (μm/min) of PLLA16k-b-PEO5k copolymer films crystallized at 110 °C, as a function of the film thickness, in linear scale.

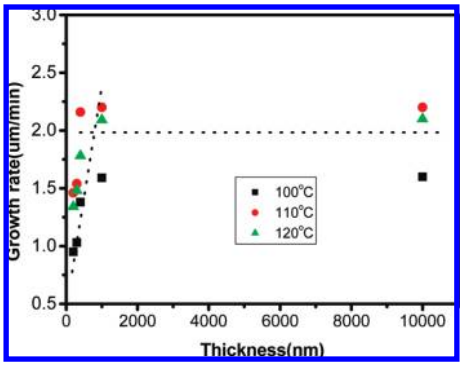

Figure 11. Radial growth rate G (μm/min) of PLLA16k-b-PEO5k copolymer films crystallized at 100, 110, and 120 °C, as a function of the film thickness, in linear scale.

morphology. In the sector [110] growth plane, the chain-folding direction is the same as the crystal growth direction. However, the chain-folding direction in the sectors with a [100] growth plane alternates between [110] sectors. In the case of the PLLA thin film, the sectors with the [100] growth plane showed some striations. They are along the main branches and parallel with each other, and the striations are nearly perpendicular to the crystal growth face, suggesting that the disordered chain (amorphous PLLA and PEO phase) packing exists in addition to the chain-folding instability. They suggested that the striations were formed due to the periodic sliding of the molecular chains along the c axis or collapse of the molecular chains along the a axis.[38] For poly[(S)-lactide], the dendritic morphology was observed in thin films below 30 nm in thickness, and hexagonal crystals were revealed in thin films of 50−100 nm thickness.[38] The asymmetric PLLA-b-PEO copolymers in our experiment can form crystalline morphology similar to that of poly[(S)-lactide], which indicates that, to some degree, the PEO block may have influence on the crystallization of PLLA similar to that in poly-[(S)-lactide].

Growth Rate. Figure 9 shows the average radical growth rate (G) of the main branches at four different film thicknesses, ~1000 nm, ~400 nm, ~300 nm, and ~200 nm, in a 100−125 °C temperature range. For each curve, it is bell shaped, which is typical for the growth rate of the polymer, as expected in this temperature range. The maximum of the growth rate is 115 °C more or less, which is identical with those of the PLLA homopolymer and its copolymers. The significant decrease of G with the film thickness is unexpected for this range of thicknesses (~200−1000 nm). The G values are too small at high temperature because it is quite difficult for nucleation to occur. We can see that the relative decrease of G as a function of film thickness is more or less the same at each T_c. The average decrease (shown in Figure 9) of G is of the order of 14% from 1000 nm to ~400 nm, of 36% from 1000 nm to ~300 nm, and of 43% when going from 1000 nm to ~200 nm. Similar observations were made for PLLA30k-b-PEO5k copolymer thin films at a temperature of 110 °C and at four thicknesses roughly from 200 nm to 1000 nm, as shown in Figure 10, but the average decrease of G is of the order of only 13% from 1000 nm to 210 nm, quite smaller than that (43%) of PLLA16k-b-PEO5k copolymer thin films, which indicates that the decrease of G with film thickness is component-dependent.

Figure 11 shows G at a certain T_c of PLLA16k-b-PEO5k copolymer as a function of film thickness. We can see that the growth rate curve contains two different parts sketched by the dotted line. In thin films ranging from 1000 nm to ~200 nm, G decreases with the film thickness, while in films with the thickness more than 1000 nm, the values of G are more or less the same. These indicate that the growth rate G is dominated by the film thickness in thin films below 1000 nm and by temperature in thick films. These data, obtained at different components and temperatures, indicate that the decrease of G with the film thickness is a general phenomenon for the PLLA-b-PEO copolymer.

Conclusions

The crystallization and morphological behaviors in thin films of asymmetric PLLA-b-PEO diblock copolymers were investigated. Dendritic superstructures stacked with single crystals were observed for asymmetric PLLA-b-PEO copolymer thin films (~200 nm−1 μm), and the fringe frame of the morphologies is hexagonal in thin films of 200−400 nm thickness. They are the cooperative results of the crystallization of the PLLA block, microphase separation between the PLLA and PEO blocks, and the effect of film thickness. The growth process of the superstructure can be classified into three steps: the growth of the main branches, the growth of the secondary side branches along the main branch, and the tertiary side branches. Two different sectors in the hexagonal superstructure, [100] and [110], were formed in terms of chain-folding and crystal growth directions. The lamellar structure was a lozenge- or truncated-lozenge-shaped single crystal of PLLA. We speculated that the formation of the single crystal was the result of the layer−layer structure driven by microphase separation.

The growth rate of dendritic morphologies that develop in thin PLLA-b-PEO copolymer films (less than 1 μm) is greatly influenced by the film thickness. Our observation shows that, as the

film thickness is decreased below 1 μm, the growth rate also decreases with, for example, ~200 nm thin PLLA16k-b-PEO5k copolymer films crystallizing nearly 2 times slower than the ~1000 nm ones. This is the result of chain diffusion and microphase separation.

Acknowledgment. This work was supported by the National Natural Science Foundation of China (20574069, 50773082, and 20490220) Programs and the Fund for Creative Research Groups (50621302), and subsidized by the Special Funds for National Basic Research Program of China (2003CB615600).